

Published in final edited form as:

Urol Oncol. 2014 January ; 32(1): 39.e1–39.10. doi:10.1016/j.urolonc.2013.04.002.

Performance of multiparametric magnetic resonance imaging in the evaluation and management of clinically low-risk prostate cancer

Seyed Saeid Dianat, M.D.^a, H. Ballentine Carter, M.D.^b, and Katarzyna J. Macura, M.D., Ph.D.^{a,b,*}

^a The Russell H. Morgan Department of Radiology and Radiological Science, The Johns Hopkins University, Baltimore, MD

^b The James Buchanan Brady Urological Institute, The Johns Hopkins University, Baltimore, MD

Abstract

Objective—The purpose of this article is to review the multiparametric magnetic resonance imaging (mMRI) of the prostate and MR-guided prostate biopsy, and their role in the evaluation and management of men with low-risk prostate cancer.

Methods—We performed a literature review based on the MEDLINE database search for publications on the role of mMRI (a) in detection and localization of prostate cancer, prediction of tumor aggressiveness and progression and (b) in guiding targeted prostate biopsy.

Results—The mMRI, particularly diffusion-weighted imaging with T2-weighted imaging, is a useful tool for tumor localization in low-risk prostate cancer as it can detect lesions that are more likely missed on extended biopsy schemes and can identify clinically significant disease requiring definitive treatment. The MR-guided biopsy of the most suspicious lesions enables more accurate and safer approach to guide enrollment into the active surveillance program. However, the MR-guided biopsy is complex. The fusion of MRI data with transrectal ultrasound for the purpose of biopsy provides a more feasible technique with documented accurate sampling.

Conclusion—Although the mMRI is not routinely used for risk stratification and prognostic assessment in prostate cancer, it can provide valuable information to guide management of men with low-risk disease. Incorporation of mMRI into the workup and monitoring of patients with low-risk prostate cancer can help discriminate clinically significant disease from indolent disease. Targeted biopsy of MR-suspicious lesions enables accurate sampling of potentially aggressive tumors that may affect outcomes.

Keywords

Prostate cancer; Multiparametric MRI; Active surveillance; Biopsy

1. Introduction

As a consequence of widespread use of prostate-specific antigen (PSA) for prostate cancer screening, high-risk prostate cancers that are amenable to curative therapy are diagnosed earlier. However, at the same time, widespread screening is also associated with false-positive results and detection and overtreatment of low-risk disease. Active surveillance (AS) of prostate cancer is a viable option for the management of low-risk disease. This approach not only reduces the risk of overtreatment of indolent disease, but also appears to provide similar disease-free outcomes when compared with immediate treatment [1]. The most widely used criteria for categorization of low-risk disease are pathologic features described as (1) Gleason 6 without any Gleason pattern 4 or 5, (2) organ-confined disease, and (3) tumor volume $<0.5 \text{ cm}^3$ [2,3].

Although Gleason 6 has been reported to be associated with disease progression after radical prostatectomy, reassessment of prostatectomy specimens revealed undergrading, understaging, and uncertain staging (intraprostatic incision), or grading (presence of tertiary pattern 4) in a setting of disease progression following radical prostatectomy. With precise histologic evaluation, the risk of disease progression after surgery in men with low-risk disease is very low (0.4%) [4].

There are wide variations in pathologic biopsy parameters used for inclusion into AS programs. However, the rate of unfavorable disease is still high and even with strictest criteria and use of 20 plus core biopsy protocol, 20% of patients are misclassified as having a low-risk disease [5].

Few nomograms have been reported to discriminate low-risk disease from clinically significant disease. The most predictive model was suggested by Chun et al. with 90% predictive accuracy of low-risk disease detection [6]. The earliest nomogram was developed by Kattan and colleagues [7]. Recently, they have incorporated imaging findings, from the magnetic resonance imaging and spectroscopy (MRI/MRSI) to the Kattan nomogram and have validated the new models. The area under the curve (AUC) increased from 0.558 to 0.741 in a base model and from 0.707 to 0.762 in another model incorporating percent of positive biopsy cores [8].

MRI has emerged as a promising tool for the evaluation of the prostate because with its high soft tissue contrast, it allows morphologic assessment of the gland, and with its capabilities to evaluate molecular and physiologic parameters of tissues, it aids in detection of metabolic, diffusion, and perfusion abnormalities associated with cancer.

Reclassification of disease in patients undergoing AS mainly occurs 1 to 2 years after the diagnosis, which is primarily owing to undersampling of the more aggressive tumor rather than progression of indolent tumor [9,10]. These sampling errors result from the lack of access to the more aggressive lesions located anteriorly in the transition zone (TZ) or blind biopsy of lesions even with systematic extended biopsy schemes. Therefore, the introduction of MR-targeted biopsy allowed a more accurate sampling of the most suspicious lesions detected on imaging.

In this article, we review the multiparametric MRI (mMRI) of the prostate and MR-guided prostate biopsy, and their role in the evaluation and management of men with low-risk prostate cancer.

2. Overview of mMRI of the prostate

2.1. Morphologic MR imaging

The morphologic imaging with T2-weighted imaging (T2WI) gives a picture of the zonal anatomy of the prostate. The peripheral zone (PZ) tumors are typically detected as low signal intensity lesions on the high signal intensity background of normal tissue on T2WI. However, T2WI alone is neither sensitive (47.8%–88.2%) nor specific (44.3%–81%) for prostate cancer detection and should be interpreted in combination with other functional MR parameters [11]. For instance, there are some benign conditions, such as hemorrhage, prostatitis, scarring, atrophy, and effects of radiation therapy, cryotherapy, or hormonal therapy, that can mimic tumors on T2WI alone. The T1-weighted imaging (T1WI) does not show details of the prostate anatomy; however, it is sensitive in detection of postbiopsy hemorrhage and is also used to define extraprostatic anatomy, such as neurovascular bundles, lymph node enlargement, and bone lesions [12].

2.2. Diffusion-weighted imaging (DWI)

DWI as one of the functional MR parameters examines the water molecule diffusivity, which is inversely related to the density of the cellular microenvironment. Cancers typically exhibit restricted diffusion owing to the high cellular density and extracellular disorganization and appear hyperintense on DWI and hypointense on the corresponding Apparent Diffusion Coefficient (ADC) map [13]. The ADC parameter is a quantitative biomarker for diffusion representing the net displacement of water molecules (expressed in mm^2/s). DWI along with T2WI improves specificity for prostate cancer detection in PZ and is particularly useful to differentiate the abnormalities owing to postbiopsy hemorrhage and benign prostatic hyperplasia (BPH) in the TZ from tumor and to detect tumor invasion to adjacent organs (bladder and seminal vesicle) [14]. It has been shown that TZ tumors show lower ADC values compared with BPH nodules and normal tissue [15]. Furthermore, the ADC value is higher in glandular-ductal tissues (glandular BPH) compared with stromal ductal tissues (stromal BPH and central gland) [16].

Ren et al. [17] have shown a significant difference in ADC values for the normal TZ, PZ, prostate cyst, BPH nodules, and prostate cancer ($P < 0.001$); with the prostate cyst having the highest ADC value, whereas the cancer foci having the lowest ADC value.

2.3. Dynamic contrast-enhanced (DCE) MRI

DCE-MRI examines the dynamic distribution of the intravenously administered contrast agent between the tissue and blood pool and determines the changes in the tumor microvasculature evoked by tumor angiogenesis. Alterations in tumor vessels include higher permeability, vascular size heterogeneity, and disorganized branching pattern [12].

Prostate cancer tissue exhibits a particular enhancement pattern characterized by faster and more intense tumor enhancement and earlier contrast agent washout compared with the normal prostate tissue [18]. In addition, DCE offers some valuable information with prognostic implication. Studies suggest a worse prognosis of disease when the number of abnormal vessels in the tumor increases [19,20].

2.4. MR spectroscopic imaging (MRSI)

MRSI provides important information about the biochemical and metabolic environment of the tissue and can detect alterations in the metabolic profile of tumor tissues [21].

Three metabolites, including choline, creatine, and citrate, are the prominent metabolites in the MR spectrum of the prostate. The citrate level reflects the glandular composition of the prostate. Thus, it is higher in the glandular BPH than the stromal-type BPH and normal PZ [21]. The citrate level lowers in cancer, especially in poorly differentiated tissue, losing its glandular properties. It is further reduced in the metastatic prostate cancer tissue [22]. However, the citrate level can also be decreased nonspecifically in prostatitis and postbiopsy hemorrhage [12].

The choline level, a composite of the phospholipid cell membrane, is elevated in prostate cancer owing to increased turnover of cell membrane during cell proliferation and higher ratio of cell surface area and cell membrane to the cellular volume in tumor cells. The elevation of the choline peak on MR spectrum of the prostate is a feature of prostate cancer; however, it can also be elevated in benign conditions such as prostatitis [12].

The MR spectroscopic profile of prostate cancer tissue is recognized by increased choline to citrate ratio or the (choline + creatine) to citrate ratio. MRSI has shown the potential for noninvasive assessment of tumor aggressiveness [23]. In addition to diagnostic yield of MRSI in combination with other parameters, it can also be useful for determination of response to neoadjuvant hormone therapy [24].

2.5. Endorectal coil

The application of endorectal coil remains controversial. When imaging at 3.0-T magnetic field strength, sufficient signal-to-noise ratio is achieved to permit a high-quality diagnostic prostate MRI without the use of endorectal coil, with comparable results to MRI at 1.5 T with endorectal coil [25]. However, spatial resolution is increased with the use of endorectal coil improving the sensitivity of MRI even at 3.0 T. Recommendations from the European consensus imply that a 16-channel pelvic-phased array (PPA) coil is the minimum requirement, whereas the combination of PPA with endorectal coil is optimal for prostate MRI providing excellent signal-to-noise ratio and clear anatomical definition of tumor borders and relationship to the capsule [26].

Previous studies emphasized the improved performance of MRI using endorectal coil for localization and staging of prostate cancer [27]. Two recent studies employed the endorectal coil at 3.0 T for prostate cancer characterization and detection of CSD in patients with low-risk disease for enrollment or follow-up in AS programs [28,29].

3. Tumor localization in low-risk disease

Early studies showed that the addition of functional imaging parameters improves the sensitivity of tumor detection. However, those early studies mostly used low-strength field scanners with a limited specificity [30].

A combination of T2WI, DWI, and DCE-MRI was reported as the best protocol for imaging of unilateral low-risk PZ cancer with sensitivity and specificity of 85% and 83%, respectively. Although the combination of T2WI and DWI is the best imaging protocol for detection of TZ tumors in unilateral low-risk disease with sensitivity and specificity of 88% and 86%, respectively [31]. However, Doo et al. [32] found that the addition of DWI to T2WI did not improve the detection of low-risk tumors (Gleason 6). This is contrary to the beneficial role of DWI combined with T2WI for detection of intermediate- and high-risk diseases (Gleason 7).

4. Prediction of tumor laterality

Hemiablative focal therapy is a potential treatment method for patients with unilateral clinically significant disease (CSD). Matsuoka et al. assessed the performance of DWI and extended combined transperineal and transrectal ultrasound (TRUS)-guided biopsy to detect unilateral CSD or any indolent disease. They demonstrated that DWI, biopsy, and the combination of the 2 can effectively rule out the presence of any cancer (either indolent or CSD) in 22.1%, 27.8%, and 43.5%, respectively, and rule out the presence of CSD in 68.4%, 72.2%, and 95.7% of lobes, respectively. Thus, they argue that a combined DWI and extended prostate biopsy can safely select candidates for hemiablative therapy [33].

Targeted focal therapy is also being investigated for targeting index lesions with consideration of the active surveillance of untreated areas harboring indolent and clinically insignificant disease [34].

Delongchamps et al. [31] reported that a portion of men with unilateral low-risk disease (34%) are upstaged or have bilateral disease on histologic examination of prostatectomy specimen. Of whom, 80% were detected by preoperative mMRI.

In another study on patients with low-to-moderate risk disease, the combination of T2WI and DWI detected bilateral disease with a sensitivity of 84.1% and specificity of 72% with the prostatectomy as the standard and showed significantly better performance than extended biopsy [35].

5. Detection of anterior/TZ prostate cancer

The anterior prostate cancers (APC), comprising approximately 21% of all types of prostate cancer, are anatomically located in anteromedial and inferior portions of TZ or the anterior horns of PZ or both [36].

These tumors are not only nonpalpable with rectal examination but also hard to detect with TRUS biopsy [37]. Moreover, TZ-directed needle biopsy does not detect the dominant TZ

lesion in approximately 80% of cases. Thus, screening needle biopsy from TZ is not a reliable method for detection of APC [38].

Furthermore, anterior prostate is the primary location of dominant nodules greater than 1 cm³ in prostatectomy specimen of patients requiring curative treatment. This was evident from the review of prostatectomy specimen of the first 10 years of inception of the AS program at our institution. Of the 48 dominant tumors, 10 tumors were greater than 1 cm³ and all were located anteriorly. However, most prostate cancers are located in the PZ posterior aspect of the prostate. The tendency of localization of large tumors in the anterior prostate highlights the need for more precise investigation of this region during the surveillance and targeted biopsy of suspicious anterior lesions [9]. Also, a subset of TZ carcinoma is associated with significant risk of extraprostatic and aggressive disease [39].

Adequate sampling of anterior aspect of the prostate still remains challenging. Prior study showed that more sets of biopsies are often required to detect anterior tumors through standard transrectal sextant biopsy and the summated tumor length in the biopsy specimen is less than the amount of tumor from equivalent size posterior tumors [40].

The combined biopsy using transperineal and transrectal approach increases the overall detection rate by 7.2% and 8.5% when compared with each method alone, respectively [41].

Given that the percentage involvement of tumor-positive biopsy cores is an inclusion criterion for AS program, it is crucial to accurately sample all the suspicious lesions of the prostate.

Early study using conventional MRI at 1.5 T for detection of TZ tumors showed the sensitivity and specificity of 42% to 52% and 79% to 88%, respectively [42].

Akin et al. [43] employed the following imaging features of TZ tumors; homogeneously low T2 signal intensity, illdefined margins, lack of capsule, lenticular shape, and invasion of anterior fibromuscular stroma (AFMS) to detect TZ tumors using T2WI at 1.5 T with a sensitivity and specificity of 75% to 80% and 78% to 87%, respectively.

It is difficult to distinguish TZ tumors from stromal hyperplasia, infarction, and prostatitis by using only T2WI. Therefore, a combination of T2WI and functional parameters is required for more accurate detection and localization of TZ tumors.

Lemaitre et al. [44] reported a median signal-intensity enhancement of 187% and an enhancement rate of 3.87%/ sec on DCE-MRI with good correlation between DCE-MRI and prostatectomy specimen for the largest surface area ($r^2 = 0.73$) and tumor volume ($r^2 = 0.69$). Tumors involving AFMS were detected by performing additional targeted biopsies based on detection of MR-suspicious lesions.

A new term 'prostatic evasive anterior tumor syndrome' (PEATS) was coined to represent a subset of anterior-predominant prostate tumor with worrisome clinical features that are missed with traditional diagnostic tools [39]. The mMRI (T2WI, DWI, and DCE-MRI) could reclassify 12 of 14 patients in AS cohort. Radical prostatectomy was performed in 7

AS patients with the specimen Gleason 3 + 4 in 4, 4 + 3 in 1, and 8/9 in 2 patients. The diagnostic yield of MRI for detection of anterior tumors was high with a positive predictive value of 87%. It was also evident that MRI can direct biopsy to anterior prostate with high degree of accuracy, and these tumors were more aggressive than expected [45]. Contrary to this study, Al-Ahmadie et al. [46] found similar pathologic outcome of anterior tumors originating from both TZ and anterior PZ.

Although mMRI is not recommended for routine disease monitoring in patients in AS based on the latest guideline by the National Comprehensive Cancer Network, it can be considered to exclude anterior cancer if PSA level rises and systematic prostate biopsy is negative [47].

In addition, MR-guided biopsy and fusion MR-TRUS-guided biopsy of suspicious lesions detected on MRI are promising approaches for more accurate sampling of the most suspicious lesions [48,49].

6. Prediction of prognostic outcome

Endorectal MRI has been shown to be useful for prediction of prognosis of intermediate- and high-risk diseases. It appears that radiologic distinction of T3 vs. T2 disease is predictive of a significantly worse biochemical outcome in patients with intermediate- and high-risk prostate cancers [50].

The predictive value of mMRI for prognostic outcome of low-risk patients eligible for AS has not been widely studied. Tumor inappreciation at imaging is part of definition of stage T1 disease. Cabrera et al. studied the significance of radiologic distinction of T2 vs. T1 disease in prognostic outcome of AS patients. Tumor appearance on MRI and MRSI on 1.5-T scanners was not a prognostic factor for biochemical outcome. It was noteworthy that the baseline PSA level and Gleason score were not prognostic factors either for biochemical outcome in this cohort [51].

In another study, Guzzo et al. [52] examined the relationship between tumor identification on T2WI and adverse pathologic outcome in a group of patients who underwent radical prostatectomy but met the qualification criteria of AS. They reported that discrete tumor identification on endorectal MRI was not associated with adverse pathologic findings such as tumor volume, extracapsular extension, Gleason upgrading, seminal vesicle invasion, or positive surgical margin rate.

Missing the high-grade tumors on needle biopsy and misclassification of patients in AS program is a worrisome issue that provokes anxiety for both the patient and physician. Despite of stringent criteria, there are 16% to 42% of cases with low-risk disease on initial biopsy that are misclassified as AS eligible and have unfavorable pathologic features on prostatectomy specimen [53]. Furthermore, there is a significant number of patients who show upgraded or upstaged disease at repeat (confirmatory) biopsy [54].

Vargas et al. [55] investigated the performance of endorectal MRI to predict findings on confirmatory biopsy in AS patients. Disease was upgraded in 79 of 388 (20%) patients on confirmatory biopsy. They analyzed MR images and scored lesions on a 5-point scoring

system (1—definitely no tumor to 5—definitely tumor). The MRI score of 5 was highly predictive of disease upgrading on confirmatory biopsy (sensitivity 0.87–0.98). On the contrary, MRI scores of 2 or less showed a high negative predictive value (0.96–1.0) and specificity (0.95–1.0) for disease upgrading on confirmatory biopsy. It appeared that adding the endorectal MRI to initial clinical evaluation can be useful for more accurate assessment of eligibility of patients for AS program.

In another study by Margel et al. [56], the risk of reclassification among AS patients based on confirmatory biopsy and the PSA density was significantly higher among men with lesions larger than 1 cm detected on mMRI. Anatomical location of suspicious lesions on MRI was in agreement with confirmatory biopsy for 92% of lesions and more than half of them were located in the anterior TZ. On the contrary, the risk of reclassification on repeat biopsy is extremely low (3.5%) in patients with no suspicious lesion on MRI [56].

7. Tumor grading

In a study by Tamada et al. [57], ADC values in PZ tumors are in significant negative correlation with tumor Gleason score ($r = 0.497$). Similarly, Doo et al. [32] reported that the mean ADC value of tumors with Gleason 7 or higher ($779.4 \times 10^6 \text{ mm}^2/\text{s}$) is significantly lower than that of low-grade tumors with Gleason 6 ($874.6 \times 10^6 \text{ mm}^2/\text{s}$). Another study documented a significant negative correlation between the ADC values and cellular density ($r = -0.50$); cancer tissues with lower ADC values have higher cell density. The primary Gleason grade (the most common pattern of cancer cells in the lesion) was in moderate but not statistically significant negative correlation with ADC ($r = -0.335$) [58].

Recently, the suspicion of cancer on T2WI and DWI has been reported in association with adverse pathology outcome in patients undergoing radical prostatectomy. It was demonstrated that patients with no suspicious findings on T2WI and DWI had decreased risk of Gleason 7 or stage pT3 disease among patients eligible for AS who underwent radical prostatectomy [59].

Quantitative parameters of DCE-MRI have not been shown to correlate with the tumor grade or vascular endothelial growth factor (VEGF) expression as a molecular marker of angiogenesis. However, the contrast agent back-flow rate constant (k_{ep}) (washout) parameter was positively correlated with mean blood vessel count and mean vessel area fraction parameters estimated from prostate cancer [60].

Computer-aided diagnosis (CAD) provides quantitative values for mMRI parameters. A recent study showed the role of combining the 10th percentile ADC, average ADC, and T2-weighted skewness of MR-suspicious lesion for differentiation of malignant from normal prostate tissue. Authors reported a moderate correlation of ADC and vascular permeability (K^{trans}) values with Gleason score. The DCE parameter (K^{trans}) was derived from the high temporal resolution imaging (rapid postcontrast imaging series) [61].

The diagnostic performance of MRSI is improved with higher Gleason tumors. In a study by Zakian et al. [62], MRSI had higher sensitivity of 89.5% for detection of tumors with Gleason 8 or above compared with the sensitivity of 44.4% for detection of low-grade

tumors (Gleason 6). In addition, there was a trend for the correlation of metabolic ratio with tumor grade. It appeared that mean (Cho + Cr) to Cit ratio of tumor is able to discriminate low-grade tumors (Gleason 6) from higher-grade tumors that are not eligible for AS.

8. Targeted prostate biopsy

The accurate and adequate prostate sampling is crucial for determination of both patient eligibility for AS and disease monitoring. The importance of immediate repeat biopsy was evident in a study from Memorial Sloan-Kettering Cancer Center. In this study, repeat targeted biopsy in 3 months of initial biopsy session revealed upstaging and upgrading in 27% of patients eligible for AS. Authors recommended the immediate repeat biopsy for discrimination of best candidates of AS [54].

There is higher rate of prostate cancer detection by using saturation biopsy (24 cores) in patients with negative standard biopsy but persistent elevated PSA level [63]. However, there is no significant difference between transrectal and transperineal approaches regarding cancer detection after prior negative biopsy [64]. Transperineal ultrasound-guided template saturation biopsy has also been examined as a sampling method in patients with at least 2 previous negative TRUS biopsy. In the study by Mabjeesh et al. [65], prostate cancer was detected in 26% of patients, and high-grade tumors (Gleason 7) were identified in 46% of the diagnosed patients. Most of the tumors (83.3%) were located in the anterior zones of the gland indicating the high yield of transperineal approach to detect high-grade tumors and offer the need for curative treatment after several negative TRUS biopsy sessions.

The early study on the diagnostic yield of MRI-guided transrectal biopsy did not reveal promising results. Singh et al. [66] found that DCE-MRI-directed biopsy could not significantly improve the cancer detection rate compared with the repeat TRUS biopsy in patients with more than 1 previous negative biopsy and persistent elevated PSA level.

Although the mMRI can detect a considerable number of lesions that can be subsequently sampled by targeted biopsy, the performance to detect tumors differs based on the criteria used to define targets on mMRI. Vargas et al. [67] investigated the performance of combination of T2WI and MRSI to detect tumors in patients with clinically low-risk prostate cancer who underwent prostatectomy. The sensitivity to detect Gleason 6 and 7 tumors was 0.52 to 0.69 and 0.77 to 0.88, respectively. As far as size classification is concerned, the sensitivity to detect tumors larger than 0.5 cm³ but smaller than 1 cm³ was 0.64 to 0.77.

Hambrock et al. [48] reported the improved diagnostic yield of multiparametric (T2WI, DWI, and DCE) MR-guided transrectal biopsy (MR-GB) in patients with increased PSA level and 2 or more prior negative TRUS biopsies. Cancer detection rate was 59% in this cohort, which was significantly higher than the matched TRUS biopsy population (22% and 15% at second and third TRUS biopsy sessions, respectively). MR-GB exhibited an improved cancer detection rate in all PSA subgroups, and for prostate volume and PSA density. However, the superior result was not statistically significant in patients with PSA level greater than 20 ng/ml, large prostates (>65 cc), and PSA density less than 0.15 and greater than 0.5 ng/ml/cc. Furthermore, most of the patients (93%) with tumor detected on MR-GB harbored CSD, and only 3 of 40 diagnosed patients were eligible for AS. This study

revealed the beneficial role of MR-GB to detect CSD, which requires active treatment [48]. The subsequent report from this group revealed that the majority of detected cancers (87%) were clinically significant. Only 9 of 156 men with negative MRGB were diagnosed with prostate cancer at 5-month follow-up, of whom, 7 patients (78%) harbored CSD [68].

In another study, authors explored the performance of MR-GB directed to the most restricted diffusion on DWI to detect the highest Gleason grade tumor in another cohort. MR-GB could detect 18 of 22 (81.8%) tumors with highest Gleason 4 and 5. This individual-based risk stratification could be employed for better evaluation of candidates for AS and offer the need for curative treatment in patients with high-grade tumors [69].

Haffner et al. described a study where targeted biopsy of suspicious lesions on qualitative DCE-MRI was shown to detect 16% more grade 4/5 tumors and better quantified the cancer length in comparison with the systematic TRUS biopsy [70].

Recently, the performance of multiparametric (T2WI, DWI, and DCE) MR-guided transperineal biopsy was compared with systematic transperineal template-guided prostate biopsy in a group of patients with suspicious-lesion on mMRI without endorectal coil at 1.5 T or 3.0 T. Higher but not significantly different number of CSD was detected by systematic template-guided biopsy (62% vs. 57%); however, systematic biopsy detected higher number of insignificant disease (17% vs. 9.3%, $P = 0.02$). Authors concluded that MR-targeted transperineal biopsy was a promising technique to detect CSD with a lower rate for insignificant disease detection and a fewer number of cores [71].

Computer-simulation study revealed significantly better performance of transperineal MR-targeted biopsy compared with 12-core TRUS biopsy for risk stratification of biopsy specimens (74% vs. 24%). High-risk prostate biopsy criteria included maximum cancer-core length (MCCL) of more than 6 mm and more than 50% positive cores. Targeted biopsies were of higher MCCL and higher percentage of positive cores compared with systematic TRUS biopsy [72].

Given the heterogeneous features of patients enrolled and different designs of these studies, the comparison of techniques and interpretation of results are challenging and subject to bias.

Despite the usefulness of MR-GB, it is limited by the cost, the time, and the need to be performed in a real time inside the MR scanner. The time of MR-GB varies from 30 minutes to 2 hours, typically lasting more than an hour [73]. The protocols differ in the need of local anesthesia; procedures are done with the periprostatic block and may involve sedation or even general anesthesia. Fig. 1 shows an example of transrectal MR-GB in a closed bore 3-T magnet using the device engineered by Kriegel and colleagues [74]. Thus, the MR-TRUS fusion approach to guidance during biopsy offers an attractive alternative to MR-GB (Fig. 2) and different designs have been proposed for this technique.

Real-time Virtual Sonography (RVS) is a novel fusion imaging technology that fuses real-time US images with cross-sectional images such as computed tomography (CT) or MRI volume data and then displays them on the same monitor side by side [75]. This technology

enables the clinician to visualize both registered cross-sectional images and real-time US images on the same monitor and make the diagnostic and interventional procedures under real-time US visualization of the target visible on MRI. Miyagawa et al. [75] have reported the application of the RVS system for transperineal prostate biopsy in patients with at least 1 negative TRUS biopsy and increased PSA. Targeted biopsy revealed better diagnostic performance (62/192 positive cores, 32%) compared with the random biopsy (75/833 positive cores, 9%). They concluded that this technique was cost effective and can be performed in the clinical setting.

Researchers from the National Institutes of Health reported the application of an MR-TRUS fusion system similar to RVS for transrectal prostate biopsy. In this study, mMRI (T2WI, DWI, and DCE) was employed to detect the MR-suspicious lesions and subsequently target the suspicious lesions during TRUS biopsy with electromagnetic tracking allowing the MR-suspicious lesions visualization during the real-time TRUS. Similar to the previous studies, MR-TRUS fusion-guided biopsy improved the cancer detection rate compared with that of a standard TRUS biopsy. Further studies are needed to determine the role of this platform and other fusion methods in the evaluation of potential candidates for AS and sampling of MR-suspicious lesions [76].

The most recent results of the application of MR-TRUS fusion biopsy were reported in another series of patients with at least 1 negative TRUS biopsy [77]. The use of fusion biopsy system upgraded tumors detected on standard TRUS biopsies in 28 of 73 patients (38.4%). On the contrary, systematic TRUS biopsy missed approximately half of the patients with high-grade disease (52.3%) and thus imposed a risk of delayed active treatment to men with high-grade disease. Furthermore, employing the PSAD threshold of 0.15 ng/ml to decide whether to perform the biopsy could potentially prevent unnecessary biopsies in 94 of 195 men with no effect on cancer detection [77].

Sonn et al. [78] have recently investigated the performance of MR-TRUS fusion and a mechanically assisted prostate biopsy device for targeted prostate biopsy. In this study, a relatively large number of men on AS were examined with the annual prostate biopsy protocol. Positive targeted cores had greater positive Gleason 7 or more results as compared with systematic biopsy findings (36% vs. 24%, respectively). However, 11 of 29 men (38%) with Gleason 7 or more cancer were only detected on targeted biopsy [78].

A novel stereotactic perineal prostate biopsy system with MR-US fusion has also been developed. Hadaschik et al. [79] investigated the feasibility and cancer detection using targeted biopsy. Most of the highly suspicious lesions on mMRI were tumor positive on targeted biopsy.

Recently, Mouraviev et al. [80] employed mMRI for detection of suspicious lesions in patients with increased PSA level and negative TRUS biopsy or patients with low-risk disease managed with AS protocol using a novel fusion navigation system superimposing MR-suspicious lesions to real-time TRUS for a targeted biopsy. The fusion MRTRUS-guided biopsy significantly improved the tumor detection as compared with MR-suggested TRUS-guided biopsy (46.2% vs. 33.3%, respectively). There was a similar percent of

missed cancers with fusion biopsy (30.7%) and MR-suggested TRUS biopsy (33.3%). None of the missed cancers were CSD except for 1 patient with CSD in MR-suggested TRUS biopsy group [80].

Results of a recent systematic review showed that targeted biopsy was a more efficient technique than standard 12-core biopsy with improved cancer detection and fewer cores taken from patients who had previous negative biopsy. In addition, targeted biopsy could detect CSD in 10% of men who were otherwise considered to have clinically insignificant disease [81]. As the evidence in the current literature is based on different populations (biopsy naive patients vs. previously biopsied), different methods of intervention (for imaging and biopsy), different reference standards, usually absent control groups, variable definitions for suspicious lesions on mMRI, and variable definitions of CSD, the results need to be interpreted with caution and further prospective paired cohort studies are needed to establish the role of mMRI in targeting lesions during prostate biopsy.

9. Conclusion

The mMRI, particularly DWI with T2WI, is a useful tool for tumor localization in low-risk prostate cancer and can detect lesions that are more likely missed on extended biopsy schemes. Although the mMRI is not routinely being used for risk stratification and prediction of prognosis in prostate cancer, it may provide valuable information to predict outcome of men with low-risk disease in AS programs. Incorporation of mMRI into the workup and monitoring of patients with low-risk disease can help to discriminate CSD from indolent disease. MR abnormalities elicited by prostatitis, biopsy scars, and BPH may mimic the malignant features on mMRI and make the interpretation of examination challenging. Also, mMRI may miss small cancer foci (especially $<0.5 \text{ cm}^3$) and sparse cancer. Targeted biopsy of MR-suspicious lesions enables accurate sampling of potentially aggressive tumors that may affect outcomes. Using the mMRI, a number of men with low-risk disease on biopsy are identified to harbor high-grade disease in the anterior prostate that is not adequately sampled by routine transrectal biopsy. Furthermore, some patients with unilateral disease on extended biopsy are likely to have bilateral disease on mMRI and are not eligible for focal therapy. Although, the performance of mMRI and MR-targeted biopsy requires considerable experience and specialized equipments, there has been increasing utilization of these techniques in recent years, with improved detection of clinically significant tumors as well as with high specificity in excluding significant prostate cancer. These new imaging and interventional techniques have a potential to guide management of patients considered for and followed in AS programs and further prospective studies are needed to assess the role and cost-effectiveness of applying mMRI in patients' workup.

References

1. Krakowsky Y, Loblaw A, Klotz L. Prostate cancer death of men treated with initial active surveillance: clinical and biochemical characteristics. *J Urol.* 2010; 184:131–5. [PubMed: 20478589]
2. Epstein JI, Chan DW, Sokoll LJ, et al. Nonpalpable stage T1c prostate cancer: prediction of insignificant disease using free/total prostate specific antigen levels and needle biopsy findings. *J Urol.* 1998; 160:2407–11. [PubMed: 9817393]

3. Epstein JI, Walsh PC, Carmichael M, Brendler CB. Pathologic and clinical findings to predict tumor extent of nonpalpable (stage T1c) prostate cancer. *J Am Med Assoc.* 1994; 271:368–74.
4. Miyamoto H, Hernandez DJ, Epstein JI. A pathological reassessment of organ-confined, Gleason score 6 prostatic adenocarcinomas that progress after radical prostatectomy. *Hum Pathol.* 2009; 40:1693–8. [PubMed: 19683331]
5. Ploussard G, Salomon L, Xylinas E, et al. Pathological findings and prostate specific antigen outcomes after radical prostatectomy in men eligible for active surveillance—does the risk of misclassification vary according to biopsy criteria? *J Urol.* 2010; 183:539–44. [PubMed: 20006888]
6. Chun FK, Haese A, Ahyai SA, et al. Critical assessment of tools to predict clinically insignificant prostate cancer at radical prostatectomy in contemporary men. *Cancer.* 2008; 113:701–9. [PubMed: 18553365]
7. Kattan MW, Eastham JA, Wheeler TM, et al. Counseling men with prostate cancer: a nomogram for predicting the presence of small, moderately differentiated, confined tumors. *J Urol.* 2003; 170:1792–7. [PubMed: 14532778]
8. Shukla-Dave A, Hricak H, Akin O, et al. Preoperative nomograms incorporating magnetic resonance imaging and spectroscopy for prediction of insignificant prostate cancer. *BJU Int.* 2012; 109:1315–22. [PubMed: 21933336]
9. Duffield AS, Lee TK, Miyamoto H, Carter HB, Epstein JI. Radical prostatectomy findings in patients in whom active surveillance of prostate cancer fails. *J Urol.* 2009; 182:2274. [PubMed: 19758635]
10. Porten SP, Whitson JM, Cowan JE, et al. Changes in prostate cancer grade on serial biopsy in men undergoing active surveillance. *J Clin Oncol.* 2011; 29:2795–800. [PubMed: 21632511]
11. Yakar D, Debats OA, Bomers JG, et al. Predictive value of MRI in the localization, staging, volume estimation, assessment of aggressiveness, and guidance of radiotherapy and biopsies in prostate cancer. *J Magn Reson Imaging.* 2012; 35:20–31. [PubMed: 22174000]
12. Bonekamp D, Jacobs MA, El-Khouli R, Stoianovici D, Macura KJ. Advancements in MR imaging of the prostate: from diagnosis to interventions. *Radiographics.* 2011; 31:677–703. [PubMed: 21571651]
13. Lim KS, Tan CH. Diffusion-weighted MRI of adult male pelvic cancers. *Clin Radiol.* 2012; 67:899–908. [PubMed: 22498730]
14. Kim CK, Choi D, Park BK, Kwon GY, Lim HK. Diffusion-weighted MR imaging for the evaluation of seminal vesicle invasion in prostate cancer: initial results. *J Magn Reson Imaging.* 2008; 28:963–9. [PubMed: 18821631]
15. Sato C, Naganawa S, Nakamura T, et al. Differentiation of non-cancerous tissue and cancer lesions by apparent diffusion coefficient values in transition and peripheral zones of the prostate. *J Magn Reson Imaging.* 2005; 21:258–62. [PubMed: 15723379]
16. Noworolski SM, Vigneron DB, Chen AP, Kurhanewicz J. Dynamic contrast-enhanced MRI and MR diffusion imaging to distinguish between glandular and stromal prostatic tissues. *Magn Reson Imaging.* 2008; 26:1071–80. [PubMed: 18508221]
17. Ren J, Huan Y, Wang H, et al. Diffusion-weighted imaging in normal prostate and differential diagnosis of prostate diseases. *Abdom Imaging.* 2008; 33:724–8. [PubMed: 18219519]
18. Verma S, Turkbey B, Muradyan N, et al. Overview of dynamic contrast-enhanced MRI in prostate cancer diagnosis and management. *Am J Roentgenol.* 2012; 198:1277–88. [PubMed: 22623539]
19. Erbersdobler A, Isbarn H, Dix K, et al. Prognostic value of micro-vessel density in prostate cancer: a tissue microarray study. *World J Urol.* 2010; 28:687–92. [PubMed: 19714336]
20. Mucci LA, Powolny A, Giovannucci E, et al. Prospective study of prostate tumor angiogenesis and cancer-specific mortality in the health professionals follow-up study. *J Clin Oncol.* 2009; 27:5627–33. [PubMed: 19858401]
21. Kayhan A, Fan X, Oommen J, Oto A. Multi-parametric MR imaging of transition zone prostate cancer: imaging features, detection and staging. *World J Radiol.* 2010; 2:180–7. [PubMed: 21161033]
22. Kurhanewicz J, Dahiya R, Macdonald JM, Chang LH, James TL, Narayan P. Citrate alterations in primary and metastatic human prostatic adenocarcinomas: 1H magnetic resonance spectroscopy and biochemical study. *Magn Reson Med.* 1993; 29:149–57. [PubMed: 8429778]

23. Kobus T, Vos PC, Hambrock T, et al. Prostate cancer aggressiveness: in vivo assessment of MR spectroscopy and diffusion-weighted imaging at 3T. *Radiology*. 2012; 265:457–67. [PubMed: 22843767]
24. Sciarra A, Panebianco V, Salciccia S, et al. Determination of the time for maximal response to neoadjuvant hormone therapy for prostate cancer using magnetic resonance with spectroscopy (MRSI) and dynamic contrast enhancement (DCEMR). *Urol Oncol*. 2012; 30:614–9. [PubMed: 21396849]
25. Sosna J, Pedrosa I, Dewolf WC, Mahallati H, Lenkinski RE, Rofsky NM. MR imaging of the prostate at 3 Tesla: comparison of an external phased-array coil to imaging with an endorectal coil at 1.5 Tesla. *Acad Radiol*. 2004; 11:857–62. [PubMed: 15354305]
26. Barentsz JO, Richenberg J, Clements R, et al. ESUR prostate MR guidelines 2012. *Eur Radiol*. 2012; 22:746–57. [PubMed: 22322308]
27. Heijmink SW, Futterer JJ, Hambrock T, et al. Prostate cancer: body-array versus endorectal coil MR imaging at 3 T—comparison of image quality, localization, and staging performance. *Radiology*. 2007; 244:184–95. [PubMed: 17495178]
28. Mullins JK, Bonekamp D, Landis P, et al. Multiparametric magnetic resonance imaging findings in men with low-risk prostate cancer followed using active surveillance. *BJU Int*. 2013
29. Somford DM, Hoeks CM, Hulsbergen-van de Kaa CA, et al. Evaluation of diffusion-weighted MR imaging at inclusion in an active surveillance protocol for low-risk prostate cancer. *Invest Radiol*. 2013; 48:152–7. [PubMed: 23328910]
30. Kirkham AP, Emberton M, Allen C. How good is MRI at detecting and characterising cancer within the prostate? *Eur Urol*. 2006; 50:1163–74. [discussion 75]. [PubMed: 16842903]
31. Delongchamps NB, Beuvon F, Eiss D, et al. Multiparametric MRI is helpful to predict tumor focality, stage, and size in patients diagnosed with unilateral low-risk prostate cancer. *Prostate Cancer Prostatic Dis*. 2011; 14:232–7. [PubMed: 21423266]
32. Doo KW, Sung DJ, Park BJ, et al. Detectability of low and intermediate or high risk prostate cancer with combined T2-weighted and diffusion-weighted MRI. *Eur Radiol*. 2012; 22:1812–9. [PubMed: 22466514]
33. Matsuoka Y, Numao N, Saito K, et al. Combination of diffusion-weighted magnetic resonance imaging and extended prostate biopsy predicts lobes without significant cancer: application in patient selection for hemiablativ focal therapy. *Eur Urol*. 2012 [Epub ahead of print].
34. Bott SR, Ahmed HU, Hindley RG, Abdul-Rahman A, Freeman A, Emberton M. The index lesion and focal therapy: an analysis of the pathological characteristics of prostate cancer. *BJU Int*. 2010; 106:1607–11. [PubMed: 20553262]
35. Jeong IGKJK, Cho KS, You D, et al. Diffusion-weighted magnetic resonance imaging in patients with unilateral prostate cancer on extended prostate biopsy: predictive accuracy of laterality and implications for hemi-ablative therapy. *J Urol*. 2010; 184:1963–9. [PubMed: 20851437]
36. Bouye S, Potiron E, Puech P, Leroy X, Lemaitre L, Villers A. Transition zone and anterior stromal prostate cancers: zone of origin and intraprostatic patterns of spread at histopathology. *Prostate*. 2009; 69:105–13. [PubMed: 18850578]
37. Terris MK, Freiha FS, McNeal JE, Stamey TA. Efficacy of transrectal ultrasound for identification of clinically undetected prostate cancer. *J Urol*. 1991; 146:78–83. [PubMed: 1711589]
38. Haarer CF, Gopalan A, Tickoo SK, et al. Prostatic transition zone directed needle biopsies uncommonly sample clinically relevant transition zone tumors. *J Urol*. 2009; 182:1337–41. [PubMed: 19683261]
39. Shannon BA, McNeal JE, Cohen RJ. Transition zone carcinoma of the prostate gland: a common indolent tumour type that occasionally manifests aggressive behaviour. *Pathology*. 2003; 35:467–71. [PubMed: 14660095]
40. Bott SR, Young MP, Kellett MJ, Parkinson MC. Anterior prostate cancer: is it more difficult to diagnose? *BJU Int*. 2002; 89:886–9. [PubMed: 12010233]
41. Watanabe M, Hayashi T, Tsushima T, Irie S, Kaneshige T, Kumon H. Extensive biopsy using a combined transperineal and transrectal approach to improve prostate cancer detection. *Int J Urol*. 2005; 12:959–63. [PubMed: 16351651]

42. Li H, Sugimura K, Kaji Y, et al. Conventional MRI capabilities in the diagnosis of prostate cancer in the transition zone. *Am J Roentgenol*. 2006; 186:729–42. [PubMed: 16498100]
43. Akin O, Sala E, Moskowitz CS, et al. Transition zone prostate cancers: features, detection, localization, and staging at endorectal MR imaging. *Radiology*. 2006; 239:784–92. [PubMed: 16569788]
44. Lemaitre L, Puech P, Poncelet E, et al. Dynamic contrast-enhanced MRI of anterior prostate cancer: morphometric assessment and correlation with radical prostatectomy findings. *Eur Radiol*. 2009; 19:470–80. [PubMed: 18758786]
45. Lawrentschuk N, Haider MA, Daljeet N, et al. Prostatic evasive anterior tumours: the role of magnetic resonance imaging. *BJU Int*. 2010; 105:1231–6. [PubMed: 19817743]
46. Al-Ahmadie HA, Tickoo SK, Olgac S, et al. Anterior-predominant prostatic tumors: zone of origin and pathologic outcomes at radical prostatectomy. *Am J Surg Pathol*. 2008; 32:229–35. [PubMed: 18223325]
47. Network NCC. NCCN guidelines.. Prostate Cancer version 1. Dec 11. 2013 2012 Version 1.2013 Available at: http://www.nccn.org/professionals/physician_gls/pdf/prostate.pdf
48. Hambrock T, Somford DM, Hoeks C, et al. Magnetic resonance imaging guided prostate biopsy in men with repeat negative biopsies and increased prostate specific antigen. *J Urol*. 2010; 183:520–7. [PubMed: 20006859]
49. Singh AK, Kruecker J, Xu S, et al. Initial clinical experience with real-time transrectal ultrasonography-magnetic resonance imaging fusion-guided prostate biopsy. *BJU Int*. 2008; 101:841–5. [PubMed: 18070196]
50. D'Amico AV, Whittington R, Malkowicz B, et al. Endorectal magnetic resonance imaging as a predictor of biochemical outcome after radical prostatectomy in men with clinically localized prostate cancer. *J Urol*. 2000; 164:759–63. [PubMed: 10953141]
51. Cabrera ARCFV, Westphalen AC, Lu Y, et al. Prostate cancer: is inapparent tumor at endorectal MR and MR spectroscopic imaging a favorable prognostic finding in patients who select active surveillance? *Radiology*. 2008; 247:444–50. [PubMed: 18430877]
52. Guzzo TJ, Resnick MJ, Canter DJ, et al. Endorectal T2-weighted MRI does not differentiate between favorable and adverse pathologic features in men with prostate cancer who would qualify for active surveillance. *Urol Oncol*. 2012; 30:301–5. [PubMed: 21856187]
53. Ploussard G, Epstein JI, Montironi R, et al. The contemporary concept of significant versus insignificant prostate cancer. *Eur Urol*. 2011; 60:291–303. [PubMed: 21601982]
54. Berglund RK, Masterson TA, Vora KC, Eggener SE, Eastham JA, Guillonneau BD. Pathological upgrading and up staging with immediate repeat biopsy in patients eligible for active surveillance. *J Urol*. 2008; 180:1964–7. [PubMed: 18801515]
55. Vargas HA, Akin O, Afaq A, et al. Magnetic resonance imaging for predicting prostate biopsy findings in patients considered for active surveillance of clinically low risk prostate cancer. *J Urol*. 2012; 188:1732–8. [PubMed: 23017866]
56. Margel D, Yap SA, Lawrentschuk N, et al. Impact of multiparametric endorectal coil prostate magnetic resonance imaging on disease reclassification among active surveillance candidates: a prospective cohort study. *J Urol*. 2012; 187:1247–52. [PubMed: 22335871]
57. Tamada T, Sone T, Jo Y, et al. Apparent diffusion coefficient values in peripheral and transition zones of the prostate: comparison between normal and malignant prostatic tissues and correlation with histologic grade. *J Magn Reson Imaging*. 2008; 28:720–6. [PubMed: 18777532]
58. Zelhof B, Pickles M, Liney G, et al. Correlation of diffusion-weighted magnetic resonance data with cellularity in prostate cancer. *BJU Int*. 2009; 103:883–8. [PubMed: 19007373]
59. Borofsky MS, Rosenkrantz AB, Abraham N, Jain R, Taneja SS. Does suspicion of prostate cancer on integrated T2 and diffusion-weighted MRI predict more adverse pathology on radical prostatectomy? *Urology*. 2013
60. Oto A, Yang C, Kayhan A, et al. Diffusion-weighted and dynamic contrast-enhanced MRI of prostate cancer: correlation of quantitative MR parameters with Gleason score and tumor angiogenesis. *Am J Roentgenol*. 2011; 197:1382–90. [PubMed: 22109293]

61. Peng Y, Jiang Y, Yang C, et al. Quantitative analysis of multi-parametric prostate MR images: differentiation between prostate cancer and normal tissue and correlation with Gleason score—a computer-aided diagnosis development study. *Radiology*. 2013
62. Zakian KL, Sircar K, Hricak H, et al. Correlation of proton MR spectroscopic imaging with Gleason score based on step-section pathologic analysis after radical prostatectomy. *Radiology*. 2005; 234:804–14. [PubMed: 15734935]
63. Walz J, Graefen M, Chun FK, et al. High incidence of prostate cancer detected by saturation biopsy after previous negative biopsy series. *Eur Urol*. 2006; 50:498–505. [PubMed: 16631303]
64. Abdollah F, Novara G, Briganti A, et al. Trans-rectal versus transperineal saturation rebiopsy of the prostate: is there a difference in cancer detection rate? *Urology*. 2011; 77:921–5. [PubMed: 21131034]
65. Mabjeesh NJ, Lidawi G, Chen J, German L, Matzkin H. High detection rate of significant prostate tumours in anterior zones using transperineal ultrasound-guided template saturation biopsy. *BJU Int*. 2012; 110:993–7. [PubMed: 22394668]
66. Singh AK, Krieger A, Lattouf JB, et al. Patient selection determines the prostate cancer yield of dynamic contrast-enhanced magnetic resonance imaging-guided transrectal biopsies in a closed 3-Tesla scanner. *BJU Int*. 2008; 101:181–5. [PubMed: 17922874]
67. Vargas HA, Akin O, Shukla-Dave A, et al. Performance characteristics of MR imaging in the evaluation of clinically low-risk prostate cancer: a prospective study. *Radiology*. 2012; 265:478–87. [PubMed: 22952382]
68. Hoeks CM, Schouten MG, Bomers JG, et al. Three-tesla magnetic resonance-guided prostate biopsy in men with increased prostate-specific antigen and repeated, negative, random, systematic, transrectal ultrasound biopsies: detection of clinically significant prostate cancers. *Eur Urol*. 2012; 62:902–9. [PubMed: 22325447]
69. Hambrock T, Hoeks C, Hulsbergen-van de Kaa C, et al. Prospective assessment of prostate cancer aggressiveness using 3-T diffusion-weighted magnetic resonance imaging-guided biopsies versus a systematic 10-core transrectal ultrasound prostate biopsy cohort. *Eur Urol*. 2012; 61:177–84. [PubMed: 21924545]
70. Haffner J, Lemaitre L, Puech P, et al. Role of magnetic resonance imaging before initial biopsy: comparison of magnetic resonance imaging-targeted and systematic biopsy for significant prostate cancer detection. *BJU Int*. 2011; 108:E171–8. [PubMed: 21426475]
71. Kasivisvanathan V, Dufour R, Moore CM, et al. Transperineal magnetic resonance image targeted prostate biopsy versus transperineal template prostate biopsy in the detection of clinically significant prostate cancer. *J Urol*. 2013; 189:860–6. [PubMed: 23063807]
72. Robertson NL, Hu Y, Ahmed HU, Freeman A, Barratt D, Emberton M. Prostate cancer risk inflation as a consequence of image-targeted biopsy of the prostate: a computer simulation study. *Eur Urol*. 2013
73. Pondman KM, Futterer JJ, ten Haken B, et al. MR-guided biopsy of the prostate: an overview of techniques and a systematic review. *Eur Urol*. 2008; 54:517–27. [PubMed: 18571309]
74. Krieger A, Iordachita II, Guion P, et al. An MRI-compatible robotic system with hybrid tracking for MRI-guided prostate intervention. *IEEE Trans Biomed Eng*. 2011; 58:3049–60. [PubMed: 22009867]
75. Miyagawa T, Ishikawa S, Kimura T, et al. Real-time virtual sonography for navigation during targeted prostate biopsy using magnetic resonance imaging data. *Int J Urol*. 2010; 17:855–60. [PubMed: 20807266]
76. Pinto PA, Chung PH, Rastinehad AR, et al. Magnetic resonance imaging/ultrasound fusion guided prostate biopsy improves cancer detection following transrectal ultrasound biopsy and correlates with multiparametric magnetic resonance imaging. *J Urol*. 2011; 186:1281–5. [PubMed: 21849184]
77. Vourganti S, Rastinehad A, Yerram NK, et al. Multiparametric magnetic resonance imaging and ultrasound fusion biopsy detect prostate cancer in patients with prior negative transrectal ultrasound biopsies. *J Urol*. 2012; 188:2152–7. [PubMed: 23083875]

78. Sonn GA, Natarajan S, Margolis DJ, et al. Targeted biopsy in the detection of prostate cancer using an office based magnetic resonance ultrasound fusion device. *J Urol*. 2013; 189:86–91. [PubMed: 23158413]
79. Hadaschik BA, Kuru TH, Tulea C, et al. A novel stereotactic prostate biopsy system integrating pre-interventional magnetic resonance imaging and live ultrasound fusion. *J Urol*. 2011; 186:2214–20. [PubMed: 22014798]
80. Mouraviev V, Pugnale M, Kalyanaraman B, et al. The feasibility of multiparametric magnetic resonance imaging for targeted biopsy using novel navigation systems to detect early stage of prostate cancer: the preliminary experience. *J Endourol*. 2012 [Epub ahead of print].
81. Moore CM, Robertson NL, Arsanious N, et al. Image-guided prostate biopsy using magnetic resonance imaging-derived targets: a systematic review. *Eur Urol*. 2013; 63:125–40. [PubMed: 22743165]

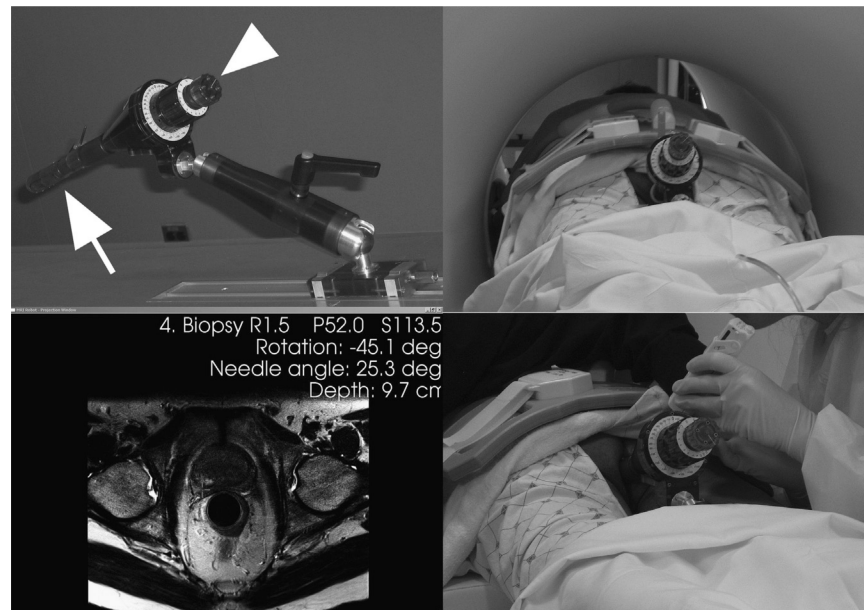


Fig. 1.

Transrectal MR-guided prostate biopsy in a closed bore 3-T magnet. Top left photograph shows an MR-compatible transrectal biopsy device with the endorectal probe (arrow) and a needle-positioning dial (arrowhead) that allows the needle to be directed to the target based on input from the targeting software. Top right photograph shows patient in prone position with the biopsy device placed in the rectum. Bottom left computer screen displays coordinates that correspond to the selected target. The software provides the following inputs: angle rotation of the probe, needle angulation, and needle depth. The dials of the biopsy device are then adjusted manually by the operator who then performs the biopsy, as is illustrated on the bottom right photograph. Note that having a patient in prone position in the small scanner gantry is limited by body habitus and uncomfortable position, and typically requires sedation.

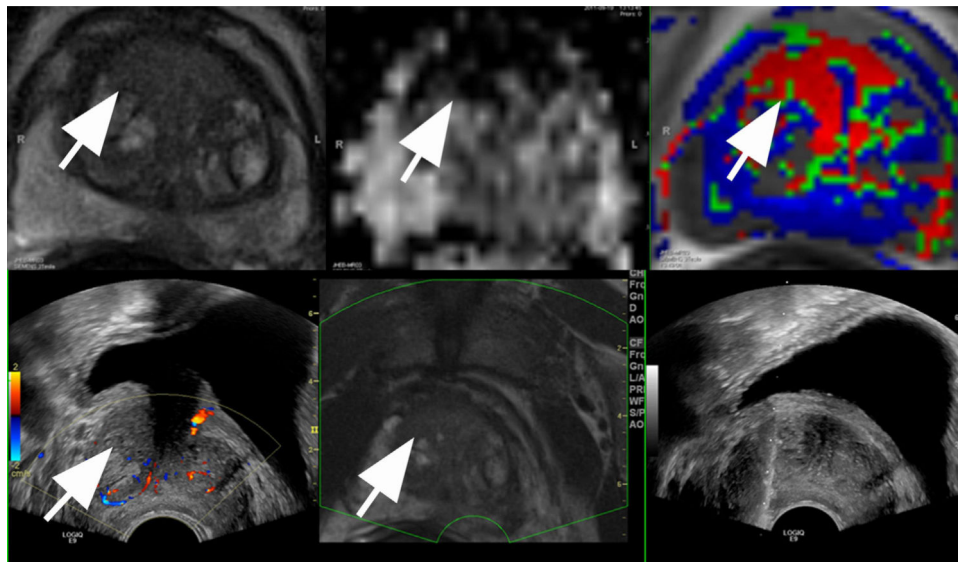


Fig. 2.

Multiparametric prostate MRI and MRI-TRUS fusion biopsy. A 76-year-old patient managed in active surveillance for a small-volume Gleason 6 prostate cancer who had persistently rising PSA level. mMRI was performed to identify clinically significant disease that could explain PSA levels. Top row images illustrate mMRI (T2, DWI, DCE-MRI) of the prostate at 3 T. T2-weighted image (top left) shows a confluent low-signal tumor in the anterior transition zone (arrow). DWI—ADC map image (top middle) shows markedly restricted (dark pixels) diffusion in the region of anterior TZ tumor (arrow). On DCEMRI K^{trans} map (top right), there is a large region (arrow) of abnormal perfusion (red) corresponding to T2WI and ADC; findings are highly suspicious for prostate cancer. Bottom row images were obtained during the MRI-TRUS fusion biopsy, where MR images were imported to the ultrasound unit and subsequently were anatomically coregistered (fused) with the real-time ultrasound images of the prostate. T2-weighted axial MR image of the prostate (bottom middle) shows the anterior tumor in TZ (arrow). Bottom left, axial ultrasound image of the prostate with color Doppler aligned anatomically with MRI shows hypoechoic region in anterior TZ corresponding to MRI (arrow). Bottom right, axial ultrasound image was captured during the biopsy, showing the needle in the anterior TZ tumor, Gleason 6. Note that MRI-TRUS fusion biopsies are performed with patient in the lateral decubitus position, in a similar fashion to the classic TRUS biopsy setup. This case illustrates the application of mMRI of the prostate for identification of suspicious target and subsequent confirmation of imaging findings with MR-targeted TRUS prostate biopsy. This approach allowed a diagnosis of clinically significant disease in a patient who was presumed low risk yet harbored moderate-volume disease in the anterior prostate that was not adequately sampled by routine TRUS biopsy. (Color version of the figure is available online.)